Attenuation of malignant phenotype of glioblastoma following a short course of the pro-oxidant combination of Resveratrol and Copper

Chaitra Bandiwadekar[1,6], Naorem Leimarembi Devi[2,3,6], Aliasgar V Moiyadi[4,6], Vikas Singh[4,6], Prakash Shetty[4,6], Sridhar Epari[5,6], Harshali Tandel[1,6], Gorantla V Raghuram[1,6], Snehal Shabrish[1,6], Pratik Chandrani[2,3,6,*], Indraneel Mittra[1,6,*]

[1]Translational Research Laboratory
Advanced Centre for Treatment, Research and Education in Cancer
Tata Memorial Centre
Kharghar, Navi Mumbai – 410210, India

[2]Computational Biology, Bioinformatics and Crosstalk Laboratory
Advanced Centre for Treatment, Research and Education in Cancer
Tata Memorial Centre
Kharghar, Navi Mumbai – 410210, India

[3]Medical Oncology Molecular Laboratory
Tata Memorial Hospital
Mumbai – 40012, India

[4]Department of Neurosurgery
Advanced Center for Treatment, Research and Education in Cancer
Tata Memorial Centre
Kharghar, Navi Mumbai – 410210, India

[5]Department of Pathology
Advanced Center for Treatment, Research and Education in Cancer
Tata Memorial Centre
Kharghar, Navi Mumbai – 410210, India

[6]Homi Bhabha National Institute, Anushakti Nagar, Mumbai –400094, India

[*] Authors for correspondence: Indraneel Mittra: imittra@actrec.gov.in

Pratik Chandrani: pchandrani@actrec.gov.in

Abstract

Background

We present a novel therapeutic approach to glioblastoma (GBM) that targets cell-free chromatin particles (cfChPs) released from dying GBM cells to aggravate the oncogenic phenotype of bystander living GBM cells. cfChPs can be deactivated by oxygen radicals (OR) generated upon admixing the nutraceuticals Resveratrol (R) and Copper (Cu). Oral administration of R-Cu leads to generation of OR which are readily absorbed to deactivate cfChPs.

Method

Ten patients with glioblastoma awaiting surgery were administered tablets containing 5.6mg of Resveratrol (R) and 560ng of Copper (Cu) q.i.d. for an average of 11.6 ± 5.37 days. Another ten patients who did not receive R-Cu acted as controls. A biopsy of the tumour tissues was taken at operation for analysis using confocal microscopy, immunofluorescence and transcriptome sequencing.

Results

Confocal microscopy of tumour sections revealed copious presence of cfChPs in the tumour microenvironment (TME) that had been released from dying GBM cells. R-Cu treatment led to deactivation / eradication of cfChPs. Eradication of cfChPs from TME led to a highly significantly reduction in Ki-67 and nine hallmarks of cancer, six immune check-points and three stem cell biomarkers. Transcriptome sequencing detected marked upregulation of pro-apoptotic and down-regulation of anti-apoptotic genes. Also detected

was down-regulation of PVRIG-2P, a homologue of immune checkpoint receptor PVRIG which is a functional analogue of PD-L1.

Conclusion

These results suggest that cfChPs released into TME are global instigators of aggressive phenotype of glioblastoma which can be attenuated by a short course of R-Cu. Trials using long term treatment with R-Cu are warranted.

ClinicalTrials.gov identifier: CTRI/2020/10/028476

Keywords

Glioblastoma, Cell-free chromatin, Cancer, Resveratrol, Copper, Oxygen radicals

Key Points

- Cell-free chromatin from dying GBM cells aggravate oncogenesis in living GBM cells
- Admixing Resveratrol with copper (R-Cu) generates oxygen radicals (OR)
- R-Cu induced OR deactivate cell-free chromatin and abates oncogenesis in GBM cells

Importance of the Study

Glioblastoma (GBM) is an incurable disease and novel therapeutic approaches are needed. Herein we present one such therapeutic approach that is non-toxic and inexpensive and targets cell-free chromatin particles (cfChPs) that are released from dying GBM cells to aggravate the oncogenic phenotype of living GBM cells. cfChPs can be deactivated by oxygen radicals (OR) generated upon combining the nutraceuticals Resveratrol (R) and Copper (Cu). Oral administration of R-Cu leads to generation of OR in the stomach which are readily absorbed to deactivate cfChPs that are released into the

tumour microenvironment (TME) of GBM. Pre-operative treatment of patients with R-Cu for ~11 days led to deactivation / elimination of cfChPs from TME. Elimination of cfChPs from TME led to a highly significantly reduction in Ki-67 and nine hallmarks of cancer, six immune check-points and three stem cell biomarkers. Prolonged treatment with R-Cu may induce GBM cells to adopt a benign phenotype.

Introduction

Despite intensive combination therapies involving surgery, radiotherapy and chemotherapy, glioblastoma remains an incurable disease with a median survival of 15 months[1]. Novel therapeutic approaches that are less traumatic and non-toxic are needed. We previously reported that cell-free chromatin particles (cfChPs) that are released from dying cancer cells can be readily internalized by bystander living cells leading to the activation of two crucial hallmarks of cancer viz. dsDNA breaks (genome instability) and inflammation[2]. Given that the concurrent induction of DNA damage and inflammation is a powerful trigger for oncogenic transformation[3,4], these findings suggested that cfChPs released into the tumour microenvironment (TME) from dying cancer cells may aggravate the malignant phenotype of the surviving cancer cells. We have also reported that the activation of DNA damage and inflammation can be abrogated by concurrent treatment with a combination of the nutraceuticals resveratrol (R) and copper (Cu) which can deactivate the cfChPs via the medium of oxygen radicals[2,5]. It was reported by Fukuhara et. al. that R functions as a catalyst to reduce Cu (II) to Cu (I) resulting in the generation of oxygen radicals which can cleave plasmid pBR322 DNA[6,7]. We have extended these findings by demonstrating that oxygen radicals produced after admixing R and Cu (R-Cu) can deactivate extracellular cfChPs by breaking down their DNA component[8,9]. When R-Cu is taken orally, oxygen radicals are generated in the stomach, which are readily absorbed and have systemic effects in the form of deactivation of extracellular cfChPs. We have reported, in pre-clinical and clinical models, that R-Cu can reduce toxicities associated with chemotherapy[10–12] and radiotherapy[5], can minimize fatality from sepsis[13,14] and downregulate multiple biomarkers of ageing and neurodegeneration[15]. No

toxic side effects attributable to R-Cu were reported in any of the above pre-clinical or clinical studies.

In the present study we tested the hypothesis that oral administration of R-Cu would lead to deactivation of cfChPs that are released into the TME from dying glioblastoma cells and prevent them from aggravating the malignant phenotype of the surviving cancer cells. Our earlier clinical studies had indicated the optimum dose of R and Cu to be 5.6 mg and 560 ng respectively[11,12,14,16]. These doses of R and Cu were combined in a bi-layered tablet formulation and used in this study. The tablets were provided for research purposes only by Inventia Healthcare Limited, Mumbai.

Material and Methods

Ethics approval

This study was approved by Institutional Ethics Committee (IEC) of Advanced Centre for Treatment, Research and Education in Cancer (ACTREC), Tata Memorial Centre (TMC) (Approval no. 3456). All participants signed a written informed consent forms which were approved by the IEC.

Patient details

Demographic information on the ten control and ten Resveratrol and Copper (R-Cu) treated patients is given in Table S1. All tumour tissues were histologically verified by a senior neuropathologist to be glioblastoma (as per WHO 2021 classification).

R-Cu tablets and dosage schedule

Bi-layer tablets containing 5.6 mg of R and 560 ng of Cu were provided by Inventia Healthcare Limited which were administered to GBM patients q.i.d. on an empty stomach. Control patient did not receive R-Cu tablets.

Sample collection

Biopsy samples of the tumour were collected at operation. One half of the sample was placed in formalin for immunofluorescence (IF) analysis and the other half was placed in RNAlater for transcriptome sequencing.

Fluorescence immune-staining and confocal microscopy

Fluorescence immune-staining using anti-DNA and anti-histone H4 antibodies followed by confocal microscopy was performed on formalin fixed paraffin embedded (FFPE) sections to detect the presence of cfChPs in TME of tumour tissues. The detailed protocol of the procedure is described by us earlier[13]. Fluorescence intensity of five randomly chosen confocal fields (~ 50 cells in each field) was recorded, and mean fluorescence intensity (MFI) (± S.E.M) was estimated.

Immunofluorescence

Indirect IF analysis on FFPE sections of tumour tissues was performed using a protocol described by us earlier[16]. The various biomarkers analyzed by IF are listed in Table S2. The table also provides information on the sources and catalogue numbers of the primary and the secondary antibodies used for IF analysis. IF analyses were done in a blinded fashion such that the examiner was unaware of the identity of the slides being analysed. One thousand cells were analysed on each slide and the percentage of cells positive for

fluorescent signals of the various biomarkers was recorded. The only exception was Annexin V where MFI per cell was recorded after analyzing one thousand cells.

Transcriptome analysis

Differential expression analysis

Raw RNA-seq FASTQ files were evaluated for quality control checks using FastQC tool (v0.12.1)[17]. Low-quality reads and adapter sequences were trimmed using Fastp[18] and the results of FastQC reports were summarized using multiQC (v1.15)[19]. Trimmed reads were then aligned to the Human GRCh38 transcriptome and Ensembl annotation v104 using Salmon (v1.5.1)[20] in a quasi-mapping-based mode, which enabled accurate transcript abundance quantification with GC bias and sequence level bias corrections. The transcript-level abundances were converted into gene-level counts using tximport (v1.18.0) package in R[21]. Differential gene expression analysis was performed using DESeq2 (v1.30.1)[22] with Wald's test for significance testing. The threshold for differential expression is set at log2fold-change (log2FC) of ±2 and adjusted p-value (padj)<0.05. These differential expressed genes (DEGs) were then visualised with a volcano plot created using EnhancedVolcano[23].

Pathway Enrichment Analysis

Pathway enrichment analysis was performed using Gene set enrichment analysis (GSEA; v4.3.3)[24] on DESeq2-normalized counts, utilising msigdb.v2023.2.Hs.symbols.gmt gene set. The analysis involved 1000 phenotype permutations and used Signal2Noise ranking metric to generate the ranked list of genes. Enrichment was evaluated based on normalised enrichment score (NES), with positive scores indicating upregulation and negative scores indicating down-regulation. A false discovery rate (FDR) q-value≤0.05

was considered statistically significant. Additionally, the genes associated with apoptosis and proteasomal degradation pathways were visualized as a network map in Cytoscape[25]. AutoAnnotate, a Cytoscape app was used to enhance visualization by labelling and grouping the pathways, thus identifying distinct functional clusters[26].

Statistical analysis

Statistical analysis was performed using two-tailed unpaired student's *t*-tests using GraphPad Prism 8 (GraphPad Software, Boston, MA, USA) and the results are expressed as mean ± SEM. The significance thresholds were: * $p<0.05$, ** $p<0.01$, *** $p<0.005$, and **** $p<0.0001$.

Results

R-Cu treatment eradicates cfChPs from TME

Confocal microscopy following fluorescent immune staining of FFPE sections using anti-DNA and anti-histone H4 revealed copious presence of cfChPs in TME of the untreated samples tissues (Fig. 1A, upper panel). Under normal circumstances the DNA (red) and histone H4 (green) fluorescent signals would be expected to be restricted to the nuclei (Fig. 1A). However, we detected extensive presence of red and green fluorescent signals outside the nuclei which upon superimposing the red and green images appeared as yellow fluorescent signals representing cfChPs. This indicated that the extensive apoptotic cell death had resulted in copious release of cfChPs in TME. The yellow fluorescent particles were virtually absent in the R-Cu treated samples indicating that R-Cu treatment had deactivated / eliminated the cfChPs from TME (Fig. 1A, lower panel). This finding is quantitatively depicted in the form of histograms which indicated a

reduction in extra-nuclear mean fluorescent intensity (MFI) in the R-Cu treated samples compared to the controls ($p < 0.01$).

R-Cu treatment down-regulates cancer biomarkers

We analyzed by IF on four groups of biomarkers which included: 1) Ki-67; 2) fifteen biomarkers representing nine hallmarks of cancer; 3) six immune check-points and 4) three stem cell markers. Ki-67 labeling is routinely used in clinical practice as a measure of proliferative index of glioblastomas[27]. We observed highly significant reduction in Ki-67 levels in the R-Cu treated samples compared with untreated samples suggesting a downward shift in the histological grade of malignancy of the tumours (Mean ± SEM = 82.09 ± 2.03 vs 56.72 ± 2.33; $p < 0.0001$) (though the morphological features like quantum of necrosis/foci of microvascular proliferation did not show any significant change) (Fig. 1B, first panel). Representative IF images of Ki-67 in control and R-Cu samples is given in Figure S1. The 15 biomarkers representing 9 hallmarks of cancer defined by Hanahan and Weinberg[3] that we analyzed are listed in Table S2. The combined results of percent cells with positive signals of the 15 biomarkers are represented as box-plot in Figure 1B (second panel). We observed a highly significant reduction in the combined results of hallmarks of cancer in the R-Cu treated samples compared to untreated controls ($p < 0.0001$). Individual IF images and box-plot results of the 15 biomarkers in treated and untreated samples is given in Figure S2. It can be observed from Figure S2 that there was highly significant reduction in the levels of individual biomarkers in the R-Cu treated groups compared to controls in 13 / 15 cases ($p < 0.0001$). The only exception was ppP53 where the p value was 0.01. The immune check-points analyzed by IF were PD-1, PD-L1, TIM-3, NKG2A, CTLA-4 and LAG3. Here again the combined results demonstrated

highly significant reduction of immune check-points in the R-Cu treated samples compared to untreated controls ($p < 0.0001$) (Fig. 1B, third panel). Individual IF images and box-plot results of the 6 immune check-points in treated and untreated samples is given in Figure S3. In all cases except CTLA-4 the p value was < 0.0001. We confirmed by IF that the 5 immune check-points viz. PD-1, TIM-3, NKG2A, CTLA-4 and LAG3 co-localized with tumour infiltrating lymphocytes marked by CD3 indicating that these immune check-points were being expressed by tumour infiltrating lymphocytes (Fig. S4).

We next analyzed three stem cell markers viz. CD133, CD44 and SOX2. Of these, the first two are cancer specific while SOX2 is a general stem cell marker. The combined box-plot results revealed a highly significant reduction in the R-Cu treated samples compared to untreated controls ($p < 0.0001$) (Fig. 1B, fourth panel). Individual IF images and box-plot results of the 3 stem cell markers in treated and untreated samples is given in Figure S5. In each case the p value was highly significant at $p < 0.0001$.

RNA-seq analysis

Quality check

Out of the 20 samples, 6 samples from each group passed the quality check and were used for RNA-seq analysis. The 12 samples were sequenced for whole transcriptome analysis, with a median coverage of 42 million reads (ranging from 30-51 million) (Table S3). FastQC was used to evaluate mean per-base quality score and per-sequence quality score of RNA-seq data. We obtained median Phred quality score above 30, confirming the high quality of RNA-seq reads (Fig. S6A & S6B). Also, the boxplot of Cook's distance distribution showed that all samples had a normalized distribution of gene expression (Fig. S6C).

Clear clustering of R-Cu transcripts

Whole transcriptome multidimensional scaling (MDS) analysis identified distinct separation between R-Cu from untreated samples (Fig. 2A). The plot indicated that samples formed a cluster (teal), showing closeness of genotype upon R-Cu treatment clearly separating them from control samples. The separation of R-Cu treated samples from control sample indicated activation of a novel transcriptional circuitry upon R-Cu treatment.

Identification of differentially expressed genes and pathways

A total of 955 differential expressed genes (DEGs) were identified through DESeq2 analysis, of which 85 genes showed upregulation with a Log2FC>2 and padj<0.05 and 870 genes showed downregulation with a Log2FC<-2 and padj<0.05 (Fig. 2B and Table S4). Gene set enrichment analysis (GSEA) was conducted to identify significantly enriched pathways in R-Cu treated samples. Notably, the upregulated genes in R-Cu treated samples included pathway involved in the insulin signaling (IGF2, IGFBP7), which is known to have tumor suppressor role in cancer by inducing apoptosis and senescence in solid tumors[28] (Fig. 2B). We also observed upregulation of extracellular matrix and related pathways (SERPINA5, CPA3, CCN3, IGFBP7, LEFTY2, SOD3 and F13A1) in R-Cu treated samples which play a role in role in modulating the extracellular matrix (Fig. 2B and Table S4). Upregulation of extracellular matrix pathways have been shown to prevent metastasis and improve patient survival[29,30]. The down-regulated pathways included intracellular ion channel genes (CFTR, CNGB1 and CNGB3) which modulate several of immunological and tumorigenic cellular processes[31] (Fig. 2B and Table S4). Significant downregulation of pathways such as metastasis and CD8 T cell chromatin

were also observed in R-Cu samples with NES<-1.5 and an FDR q-value<0.05 (Fig. 2C and 2D). Also significantly down-regulated with a log2FC of -22.77 and padj<0.05 was PVRIG-2P, a pseudogene of PVRIG, which is an evolutionary homologue of PD-L1 (Fig. 2B and Table S4)[32,33].

Complex relationship between RNA and protein turn over

We found that cancer hallmark genes *BCL2, ATM*, and immune check point genes *CTLA4, KLRC1* (coding for NKG2A) showed downregulation in whole transcriptome analysis, which was also reflected in downregulation of their corresponding proteins (Fig. 1B, S7 and S2). However, we also observed discordant regulation of several hallmark, stem cell and immune check-point genes in our transcriptome analysis (Fig. S7 and Table S4). The hallmark genes *AKT1, IL6, MYC, NFKB1, TGFB1, TP53* (coding for pp53), *VEGFA, SLC2A1* (coding for GLUT1), *CDH2* (coding for N-cadherin), *CDKN21A* (coding for p21), *VIM* (coding for Vimentin); stem cell marker genes *CD44, SOX2* and immune check point genes *HAVCR2* (coding for TIM3), *LAG3* showed increased gene expression, while hallmark genes *RAD50, CCND1*, stem cell marker genes *PROM1* (CD133), immune check point genes *PDCD1* (coding for PD-1), *CD274* (coding for PD-L1) exhibited relatively unchanged expression levels (Fig. S7). On the other hand, at a protein level, their corresponding proteins uniformly exhibited downregulation (Fig. S2 & S3). Overall, an inverse correlation of gene expression and protein expression in 19 out of 24 analyzed cancer hallmarks, immune checkpoint, and stem cell markers indicates a complex regulatory relationship involving protein synthesis, protein degradation and / or post-translational modification.

R-Cu treatment increases intrinsic apoptotic cell death

A significant upregulation in gene set of hallmark apoptosis (NES = 2.899 and nominal p-value = 0) was observed in R-Cu treated samples suggesting intense activation of intrinsic cell death (Fig. 3A). Furthermore, proteasome degradation pathway, ubiquitin proteasomal system pathway and malignant metaprogram 8 proteasomal degradation pathway were also significantly upregulated in R-Cu treated samples (Fig. 3B, 3C and 3D). Figure 3E provides a comprehensive perspective of the interconnecting network of genes involved in apoptosis and proteasomal degradation pathways. The data suggests that the combined activation of apoptosis and proteasomal degradation facilitates marked intrinsic cell death upon R-Cu treatment. Consistent with this interpretation is our IF results which showed Annexin V expression to be significantly reduced, suggesting that apoptotic cellular debris were being efficiently removed from GBM tumors via these pathways resulting in proteasomal degradation (Fig. S8). These data indicated that R-Cu treatment had led to an intense intrinsic apoptosis of glioblastoma cells and that the apoptotic cellular debris was rapidly eliminated via proteosomal degradation resulting in our detection of a reduction in Annexin V in the R-Cu treated samples (Fig. S8).

Discussion

We have shown here that a simple, non-toxic and inexpensive oral combination of Resveratrol and Copper can have profound effect on the phenotypic profile of glioblastoma. According to our hypothesis, this effect was mediated via oxygen radicals that were generated upon oral ingestion of R-Cu leading to deactivation of cfChPs in TME of glioblastoma[9,34]. Using whole transcriptome and Annexin V staining we detected

activation of extensive apoptosis in the R-Cu treated samples. A marked reduction in Bcl-2 expression in the treated samples provided further evidence of activation of apoptosis of glioblastoma cells following R-Cu treatment.

Immune staining followed by confocal microscopy of FFPE sections detected copious presence of cfChPs which had been released from the dying glioblastoma cells in TME of control samples and which were virtually eliminated via the medium of ROS following a short course of R-Cu. These data indicated that R-Cu treatment had led to an intense intrinsic apoptosis of glioblastoma cells and that the apoptotic debris was rapidly eliminated via proteosomal degradation. The latter correlated with our observation of an inverse relationship between protein expression and level of RNA transcription suggestive of efficient activation of proteasomal degradation in coordination with apoptosis[35,36]. We also observed a highly significant reduction in Ki-67, an indicator of higher tumour grade, to suggest that the tumours had been down-staged to a lower histological grade. Furthermore, significant down-regulation in hallmarks of cancer, immune check-points and stem cell markers suggested that aggressive behavior of glioblastoma were markedly attenuated following a short course of R-Cu.

Whole transcriptome sequencing of R-Cu treated glioblastoma samples detected upregulation of *IGFBP7* gene – a tumor suppressor known to inhibit proliferation and induce apoptosis and senescence[28]. Furthermore, our detection of down-regulation of metastasis related genes such as *GATA2, PKD1, NFIA* suggestive of attenuation of aggressive behavior of glioblastoma which aligns with independent reports in other cancer types[37–39].

Immunotherapy of cancer is currently a hot topic. However, these targeted therapies that are currently in use are expensive and often very toxic and are generally used one at a time. Against this backdrop, our results that a simple, inexpensive and non-toxic combination of R and Cu can simultaneously down-regulate six immune check-points is a highly significant finding. In this context, we have recently reported that cfChPs released from dying cancer cells that circulate in human blood, or those that are released from dying cancer cells, can activate immune checkpoints in human lymphocytes both *in vitro* and *in vivo*[40]. The immune check-points *PD-1, CTLA-4, LAG-3, NKG2A*, and *TIM-3* were significantly activated when human lymphocytes were treated with cfChPs that were derived from cancer patient sera. The addition of R-Cu to the culture medium led to down-regulation of all five immune check-points. These results were confirmed in vivo in mouse splenocytes upon intravenous injection of cfChPs[40]. These findings taken together with our present results would indicate that cfChPs are global instigators of immune check-points which can be down-regulated by treatment with the pro-oxidant combination of R and Cu. Thus R-Cu may offer a viable alternative to immunotherapy currently in practice in the treatment of cancer.

Our present results confirm those of our earlier exploratory study in advanced oral cancer which was primarily undertaken to determine the optimal dose for R and Cu[16]. That study, conducted prior to the availability of R-Cu tablets, used oral administration of water based suspensions of R and Cu and the optimum dose of R and Cu were adjudged to be 5.6 mg and 560 ng respectively. The bi-layered tablets used in the current study were developed on the basis of the result of this earlier study. Nonetheless, our earlier study showed that oral administration of the combination of R and Cu for 2 weeks could down-

regulate multiple hallmarks of cancer and immune check-points in advanced oral cancer[16]. The results of the earlier study and the current one suggest that cfChPs that are released from dying cancer cells into TME are global instigators for cancer hallmarks and immune checkpoints in the surviving cancer cells and are primarily responsible for the potentially lethal behavior of glioblastoma.

In summary, our study shows that oral administration of a non-toxic combination of miniscule quantities of the commonly used nutraceuticals R and Cu can have profound effects in GBM in the form of attenuation of aggressive phenotype of glioblastoma. Clinical trials of prolonged administration of R-Cu in GBM are warranted.

Ethics

This study was approved by Institutional Ethics Committee (IEC) of Advanced Centre for Treatment, Research and Education in Cancer (ACTREC), Tata Memorial Centre (TMC) (Approval no. 3456). All participants signed a written informed consent forms which were approved by the IEC.

Funding:

This study was supported by the Department of Atomic Energy, Government of India, through grant CTCTMC to the Tata Memorial Centre awarded to IM.

Conflict of Interest:

The authors declare no conflict of interest.

Authorship statement:

Conception and design: I.M., A.V.M., V.S., and P.S. Development of methodology: I.M., and P.C. Acquisition of data: C.B., N.L.D., A.V.M., V.S., P.S., S.E., H.T., G.V.R., and S.S. Analysis and interpretation of data: I.M., P.C., N.L.D., S.S., and G.V.R. Writing and review of the manuscript: I.M., P.C., N.L.D., S.S., and S.E. All authors reviewed and approved the manuscript.

Data Availability

All data are included in the manuscript. Any additional data will be made available upon reasonable request. All relevant raw data will be freely available to any researcher for noncommercial purposes on request.

Acknowledgement

We thank Ms. Ruchi Joshi for her help with some of the IF experiments and Mr. Ashish Pawar for his help in preparing the manuscript.

References

1. Thakkar JP, Dolecek TA, Horbinski C, et al. Epidemiologic and Molecular Prognostic Review of Glioblastoma. *Cancer Epidemiol Biomarkers Prev*. 2014;23(10):1985-1996. doi:10.1158/1055-9965.EPI-14-0275
2. Mittra I, Samant U, Sharma S, et al. Cell-free chromatin from dying cancer cells integrate into genomes of bystander healthy cells to induce DNA damage and inflammation. *Cell Death Discov*. 2017;3(1):17015. doi:10.1038/cddiscovery.2017.15
3. Hanahan D, Weinberg RA. Hallmarks of cancer: the next generation. *Cell*.

2011;144(5):646-674.

4. Balkwill F, Charles KA, Mantovani A. Smoldering and polarized inflammation in the initiation and promotion of malignant disease. *Cancer Cell*. 2005;7(3):211-217. doi:10.1016/j.ccr.2005.02.013

5. Kirolikar S, Prasannan P, Raghuram G V., et al. Prevention of radiation-induced bystander effects by agents that inactivate cell-free chromatin released from irradiated dying cells. *Cell Death Dis*. 2018;9(12). doi:10.1038/s41419-018-1181-x

6. Fukuhara K, Miyata N. Resveratrol as a new type of DNA-cleaving agent. *Bioorganic Med Chem Lett*. 1998;8(22). doi:10.1016/S0960-894X(98)00585-X

7. Fukuhara K, Nagakawa M, Nakanishi I, et al. Structural basis for DNA-cleaving activity of resveratrol in the presence of Cu(II). *Bioorganic Med Chem*. 2006;14(5). doi:10.1016/j.bmc.2005.09.070

8. Subramaniam S, Vohra I, Iyer A, Nair NK, Mittra I. A paradoxical relationship between Resveratrol and copper (II) with respect to degradation of DNA and RNA. *F1000Research*. 2016;4:1145. doi:10.12688/f1000research.7202.2

9. Mittra I. Exploiting the damaging effects of ROS for therapeutic use by deactivating cell-free chromatin: the alchemy of resveratrol and copper. *Front Pharmacol*. 2024;15. doi:10.3389/fphar.2024.1345786

10. Mittra I, Pal K, Pancholi N, et al. Prevention of chemotherapy toxicity by agents that neutralize or degrade cell-free chromatin. *Ann Oncol*. 2017;28(9). doi:10.1093/annonc/mdx318

11. Agarwal A, Khandelwal A, Pal K, et al. A novel pro-oxidant combination of resveratrol and copper reduces transplant related toxicities in patients receiving

high dose melphalan for multiple myeloma (RESCU 001). *PLoS One*. 2022;17(2 February). doi:10.1371/journal.pone.0262212

12. Ostwal V, Ramaswamy A, Bhargava P, et al. A pro-oxidant combination of resveratrol and copper reduces chemotherapy-related non-haematological toxicities in advanced gastric cancer: results of a prospective open label phase II single-arm study (RESCU III study). *Med Oncol*. 2022;40(1):17.
13. Mittra I, Pal K, Pancholi N, et al. Cell-free chromatin particles released from dying host cells are global instigators of endotoxin sepsis in mice. *PLoS One*. 2020;15(3):e0229017.
14. Mittra I, de Souza R, Bhadade R, et al. Resveratrol and Copper for treatment of severe COVID-19: an observational study (RESCU 002). *medRxiv*. Published online 2020:2020-2027.
15. Pal K, Raghuram G V, Dsouza J, et al. A pro-oxidant combination of resveratrol and copper down-regulates multiple biological hallmarks of ageing and neurodegeneration in mice. *Sci Rep*. 2022;12(1):17209.
16. Pilankar A, Singhavi H, Raghuram G V, et al. A pro-oxidant combination of resveratrol and copper down-regulates hallmarks of cancer and immune checkpoints in patients with advanced oral cancer: Results of an exploratory study (RESCU 004). *Front Oncol*. Published online 2022:5061.
17. Andrews S. FastQC: A Quality Control Tool for High Throughput Sequence Data. Published online 2010.
18. Chen S, Zhou Y, Chen Y, Gu J. fastp: an ultra-fast all-in-one FASTQ preprocessor. *Bioinformatics*. 2018;34(17):i884-i890.

doi:10.1093/bioinformatics/bty560

19. Ewels P, Magnusson M, Lundin S, Käller M. MultiQC: summarize analysis results for multiple tools and samples in a single report. *Bioinformatics*. 2016;32(19):3047-3048. doi:10.1093/bioinformatics/btw354

20. Patro R, Duggal G, Love MI, Irizarry RA, Kingsford C. Salmon provides fast and bias-aware quantification of transcript expression. *Nat Methods*. 2017;14(4):417-419. doi:10.1038/nmeth.4197

21. Soneson C, Love MI, Robinson MD. Differential analyses for RNA-seq: transcript-level estimates improve gene-level inferences. *F1000Research*. 2016;4:1521. doi:10.12688/f1000research.7563.2

22. Love MI, Huber W, Anders S. Moderated estimation of fold change and dispersion for RNA-seq data with DESeq2. *Genome Biol*. 2014;15(12):550. doi:10.1186/s13059-014-0550-8

23. Blighe, Kevin, Sharmila Rana and ML. EnhancedVolcano: Publication-Ready Volcano Plots with Enhanced Colouring and Labeling. *R Packag Version 1*. Published online 2019:10–18129.

24. Subramanian A, Tamayo P, Mootha VK, et al. Gene set enrichment analysis: A knowledge-based approach for interpreting genome-wide expression profiles. *Proc Natl Acad Sci*. 2005;102(43):15545-15550. doi:10.1073/pnas.0506580102

25. Shannon P, Markiel A, Ozier O, et al. Cytoscape: a software environment for integrated models of biomolecular interaction networks. *Genome Res*. 2003;13(11):2498-2504. doi:10.1101/gr.1239303

26. Kucera M, Isserlin R, Arkhangorodsky A, Bader GD. AutoAnnotate: A Cytoscape

app for summarizing networks with semantic annotations. *F1000Research*. 2016;5:1717. doi:10.12688/f1000research.9090.1

27. Xu G, Li C, Wang Y, Ma J, Zhang J. Correlation between preoperative inflammatory markers, Ki-67 and the pathological grade of glioma. *Medicine (Baltimore)*. 2021;100(36):e26750. doi:10.1097/MD.0000000000026750
28. Singh CK, Chhabra G, Ndiaye MA, et al. Quercetin-Resveratrol Combination for Prostate Cancer Management in TRAMP Mice. *Cancers (Basel)*. 2020;12(8). doi:10.3390/cancers12082141
29. Bijsmans ITGW, Smits KM, de Graeff P, et al. Loss of SerpinA5 protein expression is associated with advanced-stage serous ovarian tumors. *Mod Pathol*. 2011;24(3):463-470. doi:10.1038/modpathol.2010.214
30. Jing Y, Jia D, Wong CM, et al. SERPINA5 inhibits tumor cell migration by modulating the fibronectin-integrin β1 signaling pathway in hepatocellular carcinoma. *Mol Oncol*. 2014;8(2):366-377. doi:10.1016/j.molonc.2013.12.003
31. Peruzzo R, Biasutto L, Szabò I, Leanza L. Impact of intracellular ion channels on cancer development and progression. *Eur Biophys J*. 2016;45(7):685-707. doi:10.1007/s00249-016-1143-0
32. Whelan S, Ophir E, Kotturi MF, et al. PVRIG and PVRL2 Are Induced in Cancer and Inhibit CD8+ T-cell Function. *Cancer Immunol Res*. 2019;7(2):257-268. doi:10.1158/2326-6066.CIR-18-0442
33. Yang J, Wang L, Byrnes JR, et al. PVRL2 Suppresses Antitumor Immunity through PVRIG- and TIGIT-independent Pathways. *Cancer Immunol Res*. 2024;12(5):575-591. doi:10.1158/2326-6066.CIR-23-0722

34. Khanvilkar S, Mittra I. Copper Imparts a New Therapeutic Property to Resveratrol by Generating ROS to Deactivate Cell-Free Chromatin. *Pharmaceuticals*. 2025;18(1):132. doi:10.3390/ph18010132

35. Yuan L, Li P, Zheng Q, Wang H, Xiao H. The Ubiquitin-Proteasome System in Apoptosis and Apoptotic Cell Clearance. *Front cell Dev Biol*. 2022;10:914288. doi:10.3389/fcell.2022.914288

36. Abbas R, Larisch S. Killing by Degradation: Regulation of Apoptosis by the Ubiquitin-Proteasome-System. *Cells*. 2021;10(12). doi:10.3390/cells10123465

37. Chiang YT, Wang K, Fazli L, et al. GATA2 as a potential metastasis-driving gene in prostate cancer. *Oncotarget*. 2014;5(2):451-461. doi:10.18632/oncotarget.1296

38. Wang Z, Yuan H, Sun C, et al. GATA2 promotes glioma progression through EGFR/ERK/Elk-1 pathway. *Med Oncol*. 2015;32(4):87. doi:10.1007/s12032-015-0522-1

39. Lee JS, Xiao J, Patel P, et al. A novel tumor-promoting role for nuclear factor IA in glioblastomas is mediated through negative regulation of p53, p21, and PAI1. *Neuro Oncol*. 2014;16(2):191-203. doi:10.1093/neuonc/not167

40. Shabrish S, Pal K, Khare NK, et al. Cell-free chromatin particles released from dying cancer cells activate immune checkpoints in human lymphocytes: implications for cancer therapy. *Front Immunol*. 2024;14. doi:10.3389/fimmu.2023.1331491

Figures

Fig. 1

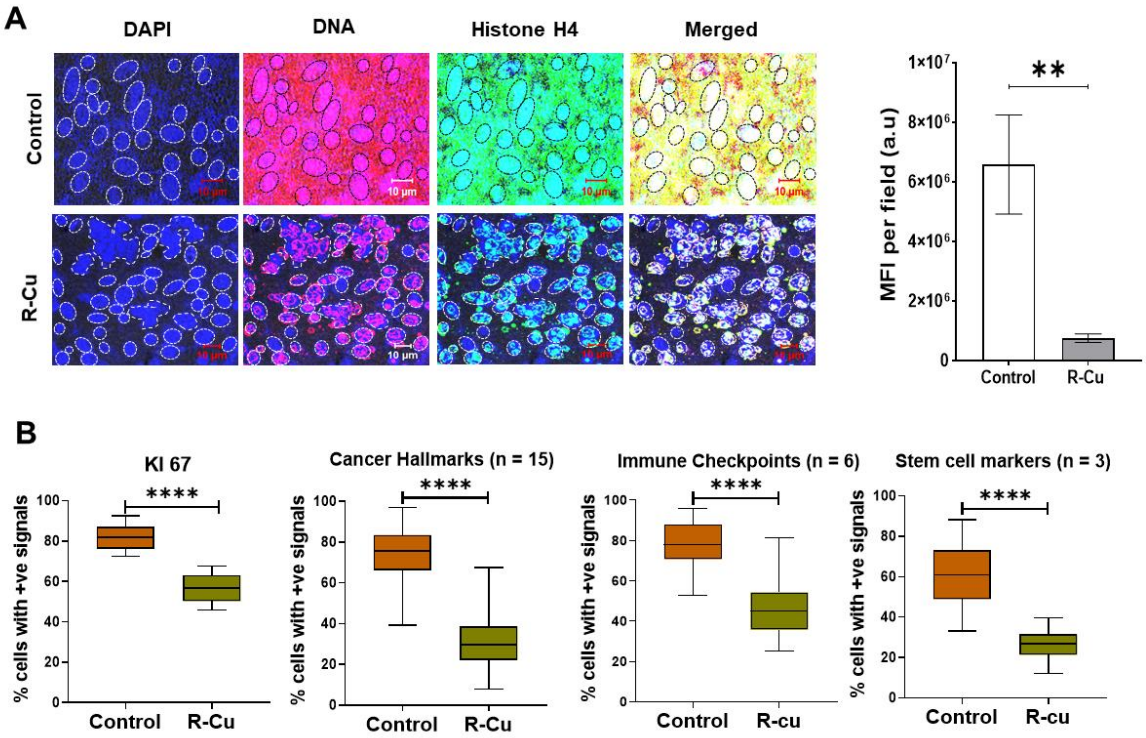

Figure 1: Representative confocal microscopy images of tumour sections to detect cfChPs in TME, and Immunofluorescence results of Ki-67, and combined results of 15 hallmarks of cancer, 6 immune check-points and 3 stem cell markers in control and R-Cu treated GBM patients. A. Representative fluorescence immuno-staining and confocal microscopy images of tumour sections of GBM samples stained with fluorescent antibodies against DNA and histone H4 and examined by confocal microscopy. Co-localizing DNA (red) and histone H4 (green) fluorescent signals generate yellow / white coloured particles that represent cfChPs. Numerous yellow / white fluorescent particles are seen outside the nucleus in the intra- or extracellular spaces in the control samples which are virtually eliminated following R-Cu treatment. Graphical representation of MFI

of extra-nuclear cfChPs (right hand image). The nuclei were gated and MFI of yellow fluorescent signals in five randomly chosen confocal fields (~50 cells per field) was estimated. The number of patient samples in control and R-Cu treated groups = 10 in each group. **B.** Boxplots representing Mean ± SEM of immunofluorescence results of Ki-67 and combined results of 15 hallmarks of cancer, 6 immune check-points and 3 stem cell markers. n = 10 patients each in control and R-Cu treated patients. ** = $p < 0.01$; **** = $p < 0.0001$.

Fig. 2

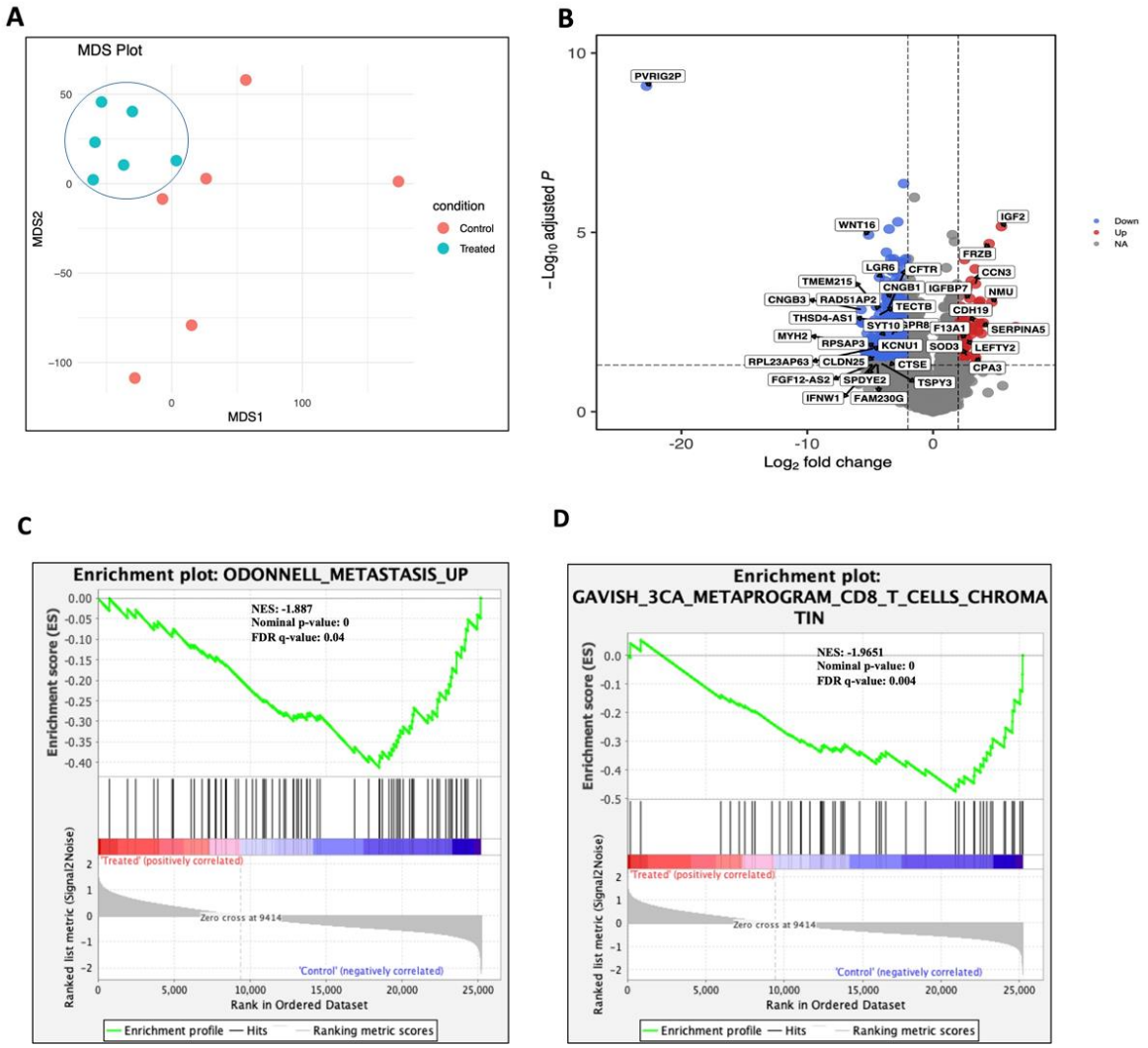

Figure 2: RNA-seq analysis of glioblastoma patients treated with Resveratrol-Copper identifies differential genes and pathways. A. MDS plot showing clusters between R-Cu treated (Teal) and untreated samples (Red). **B**. Volcano plot of statistically significant differentially expressed genes. Red dots represent up-regulated genes with log2 (fold change) > 2 and p-adjusted < 0.05, and blue dots represent down-regulated genes with log2 (fold change) < -2 and p-adjusted < 0.05. **C – D.** Gene set enrichment analysis (GSEA) plots showing de-enrichment of metastasis pathways (**C**) and cellular metaprogramming and heterogeneity pathways (**D**) respectively in R-Cu samples compared to untreated samples. For each gene set, Normalised Enrichment Score

(NES), nominal p-value, and False Discovery Rate (FDR) are shown on the plot.

Fig. 3

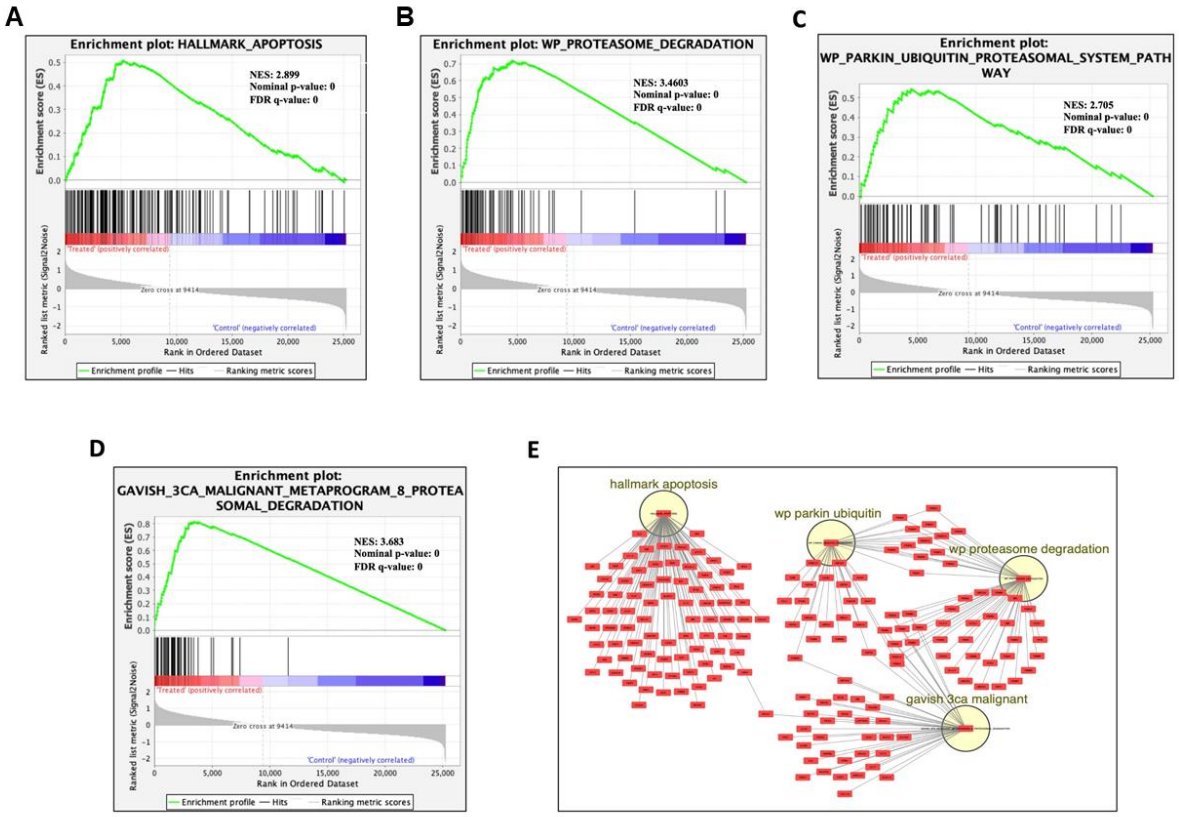

Figure 3: Transcriptomic signature indicates activation of intrinsic apoptosis and proteasomal degradation cascade upon R-Cu treatment. A. Enrichment plot generated using GSEA showing upregulation of hallmark apoptosis gene set, **B.** upregulation of proteosome degradation pathways, **C.** upregulation of Proteasomal System pathway, **D.** upregulation of Malignant Metaprogram 8 Proteasomal Degradation pathway, respectively in R-Cu treated samples. For each gene set, Normalised Enrichment Score (NES), nominal p-value, and False Discovery Rate (FDR) are shown on the plot. **E**. Network map showing genes involved in apoptosis and proteasomal degradation pathways.

Supplementary Figures

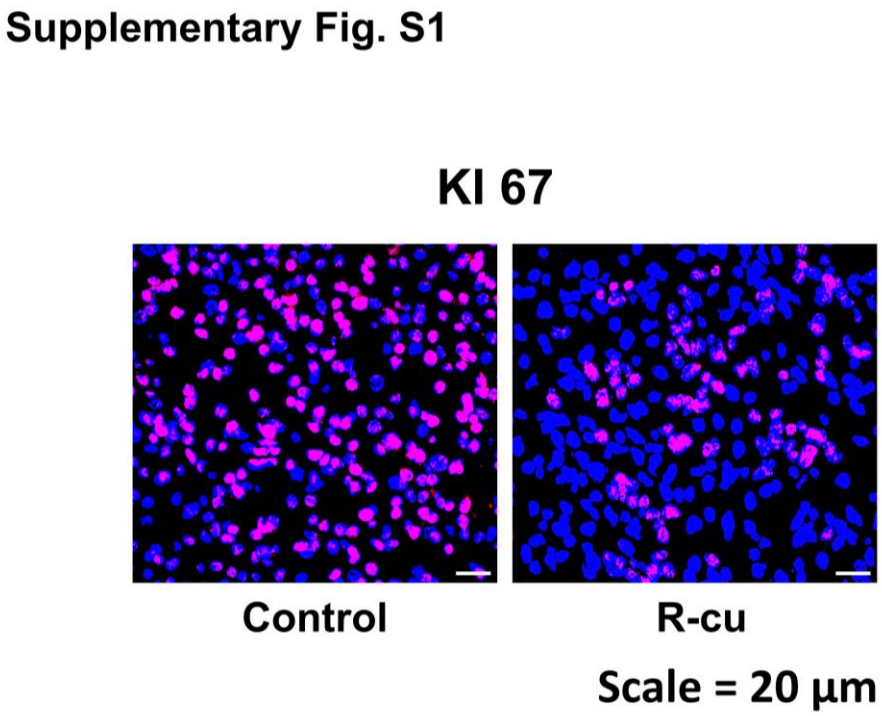

Figure S1: Representative IF images of Ki-67 in control and R-Cu treated samples. Quantitative histograms are presented in figure 1B.

Supplementary Fig. S2

Cancer hallmarks

1. Sustained Proliferation

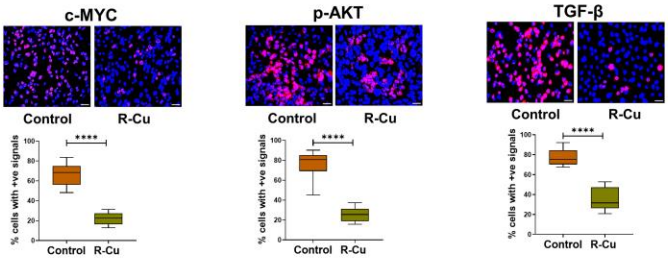

2. Evading Growth Suppressors

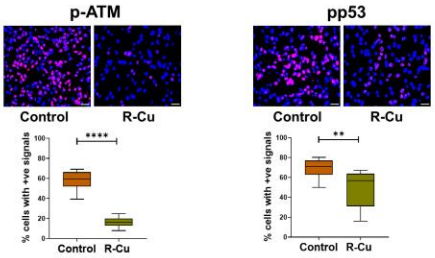

3. Tumor Promoting Inflammation

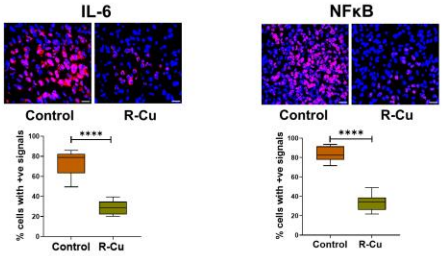

4. Enabling Replicative Immortality

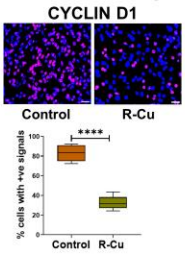

5.Inducing Angiogenesis

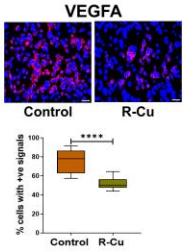

6. Deregulating Cellular Energetics

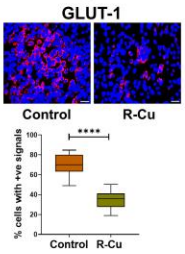

7.Activating Invasion and Metastasis

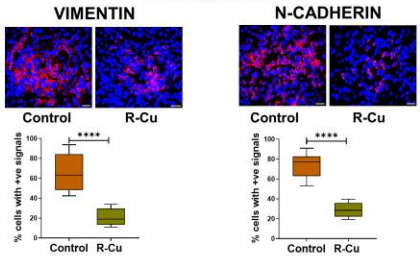

8.Genome Instability & Mutation

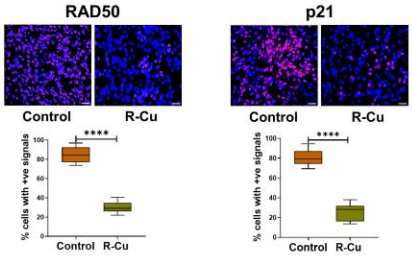

9. Resisting Cell Death

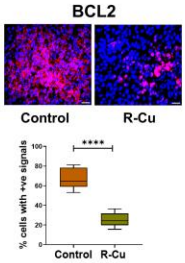

scale= 20 µm for all images

Figure S2: Representative IF images of 16 biomarkers representing 9 hallmarks of cancer and quantitative results represented as boxplots. n = 10 each in control and R-Cu groups. ** = p < 0.01; *** = p < 0.001; **** = p < 0.0001.

Supplementary Fig. S3

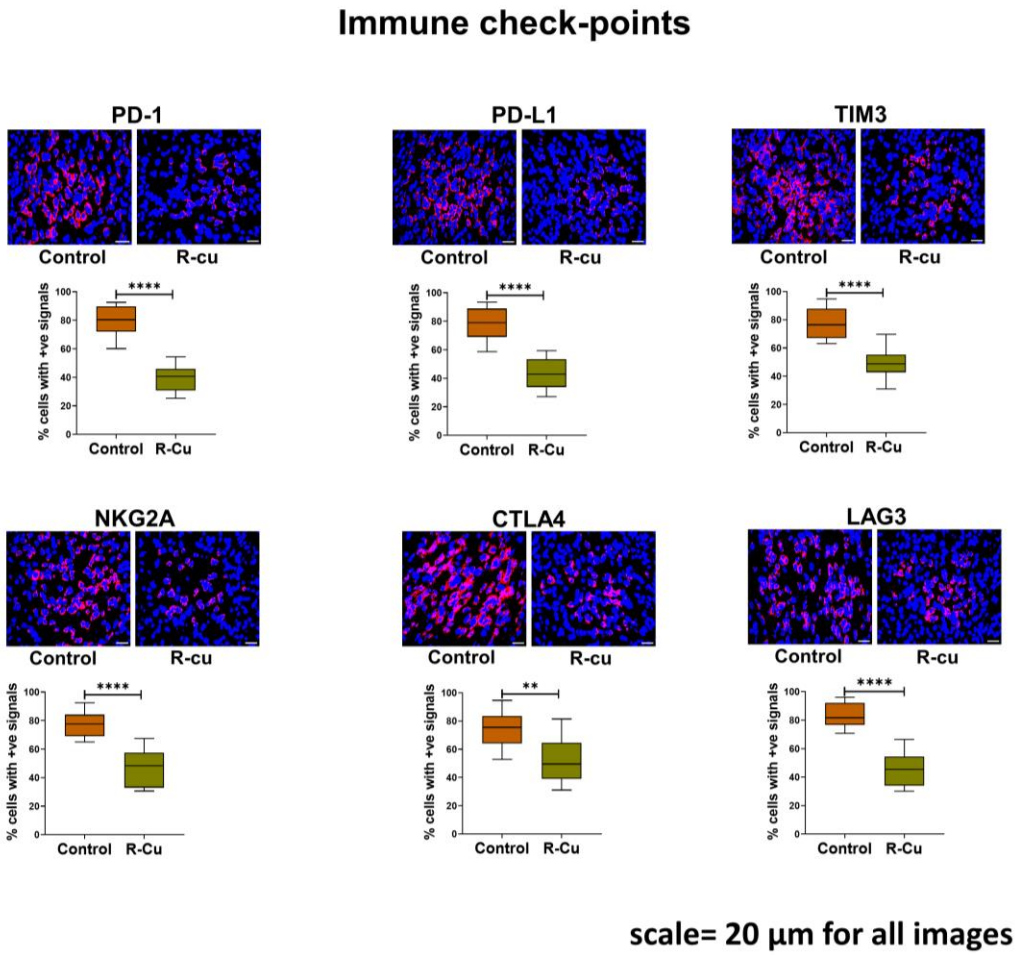

Figure S3: Representative IF images of 6 immune check-points and quantitative results represented as boxplots. n = 10 each in control and R-Cu groups. ** = p < 0.01; **** = p < 0.0001.

Supplementary Fig. S4

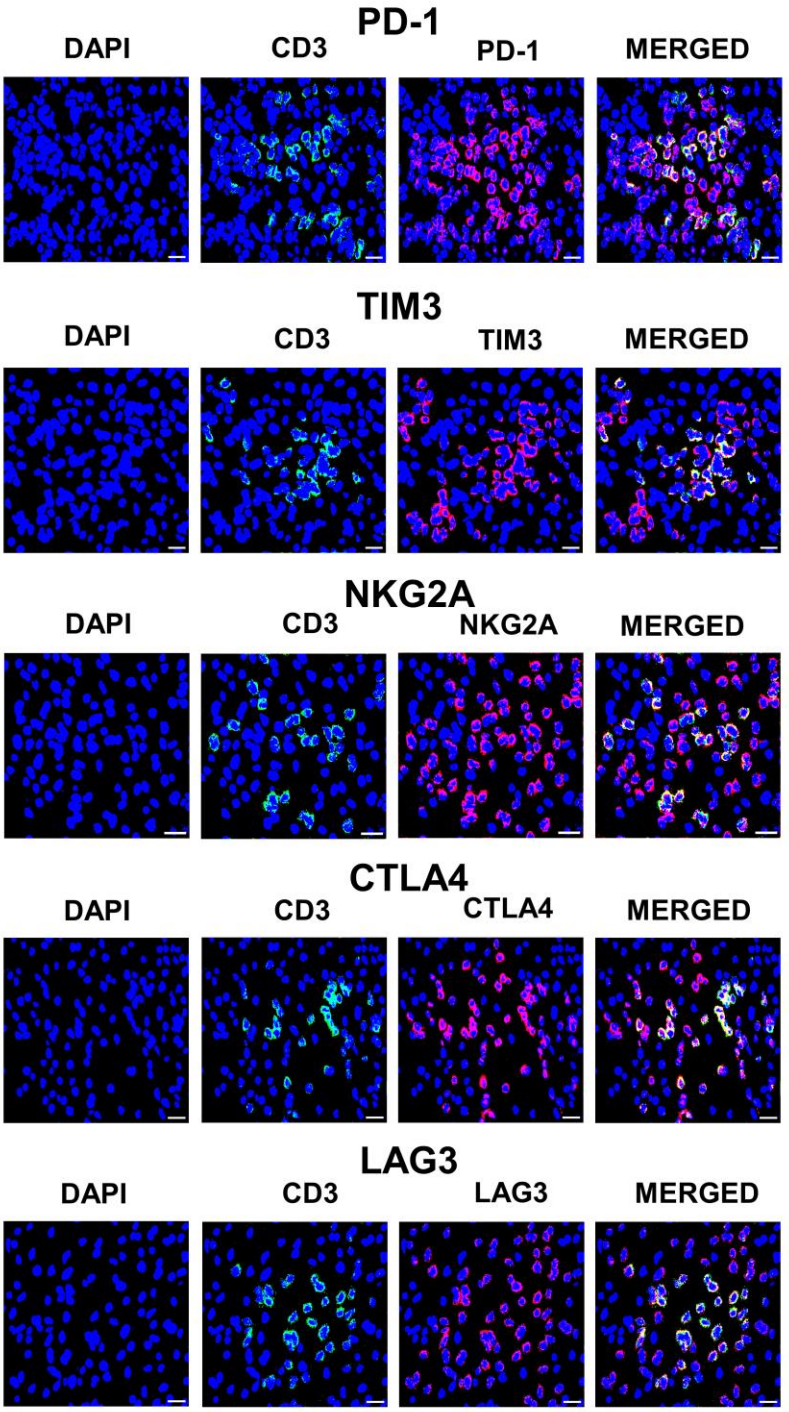

scale= 20 µm for all images

Figure S4: Representative IF images showing co-expression of various immune checkpoints by tumour infiltrating lymphocytes represented by CD3. FFPE sections of GBM tumour tissues were simultaneously immune-stained with antibodies against various immune-checkpoints and that against CD3 lymphocytes. Co-localisation of all five immune check-points and CD3 lymphocytes is clearly seen.

Supplementary Fig. S5

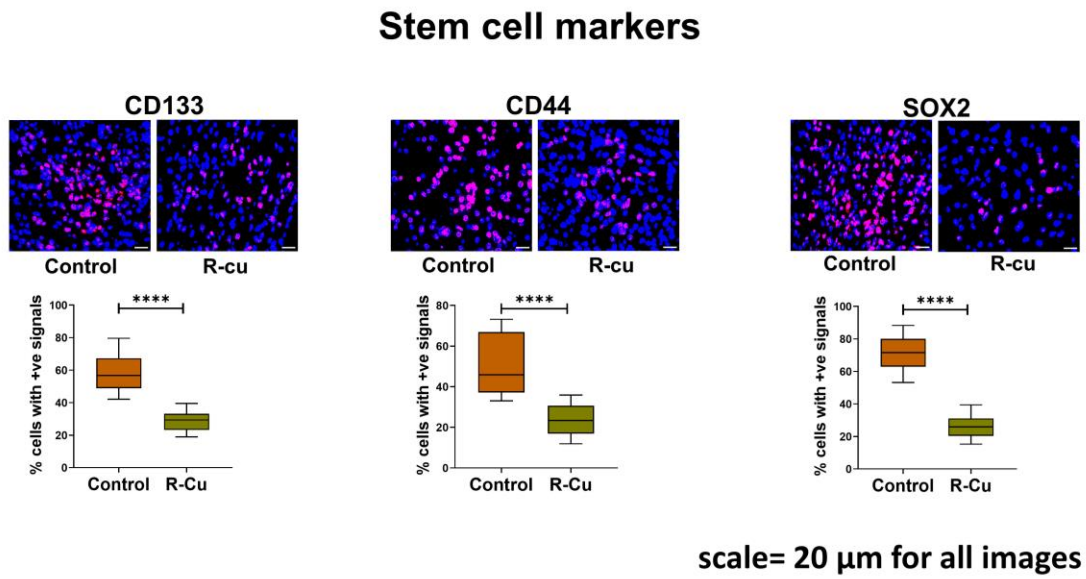

Figure S5: Representative IF images of 3 stem cell markers and quantitative results represented as boxplots. n = 10 each in control and R-Cu groups. **** = $p < 0.0001$.

Supplementary Fig. S6

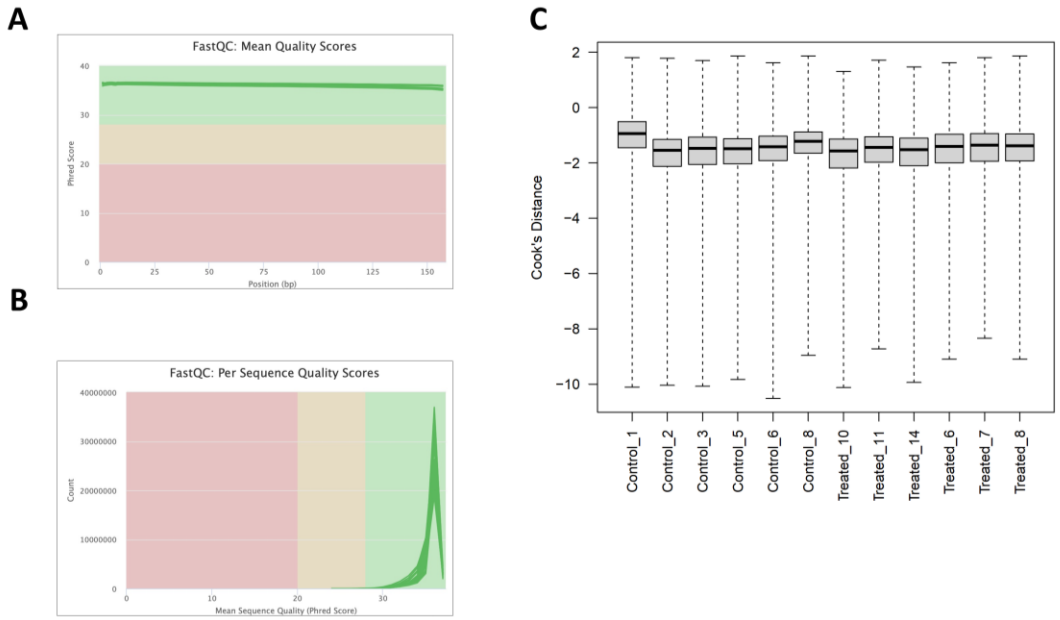

Figure S6: RNA-seq quality check and normalization. A & B FastQC plots showing mean per-base quality scores of RNA-seq data **C.** Cook's distance boxplot to visualize the data distribution post normalization

Supplementary Fig. S7

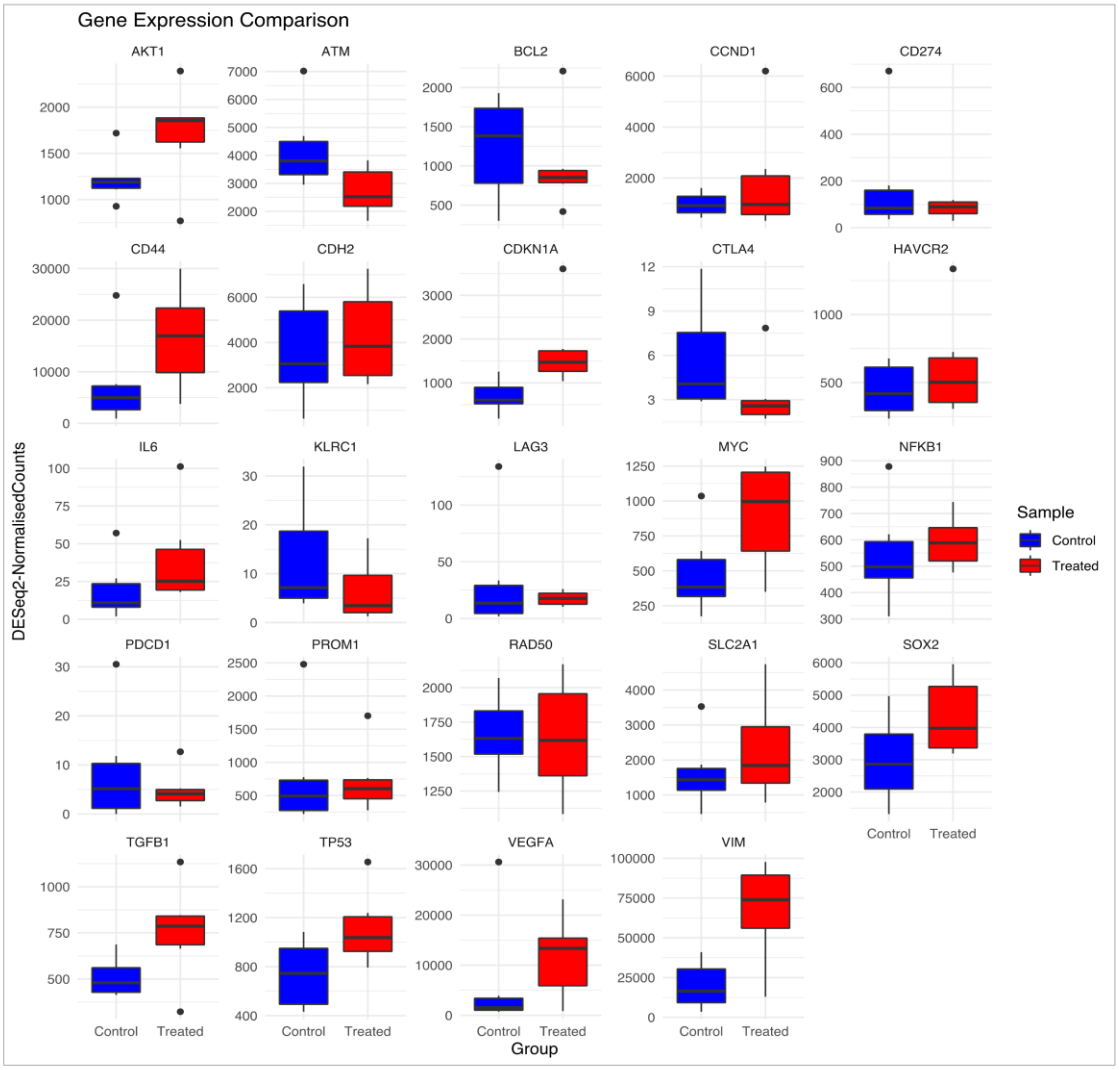

Figure S7: **Gene-wise comparison of expression in R-Cu treated and untreated samples.** Box plot representation of the selected cancer related genes

Supplementary Fig. S8

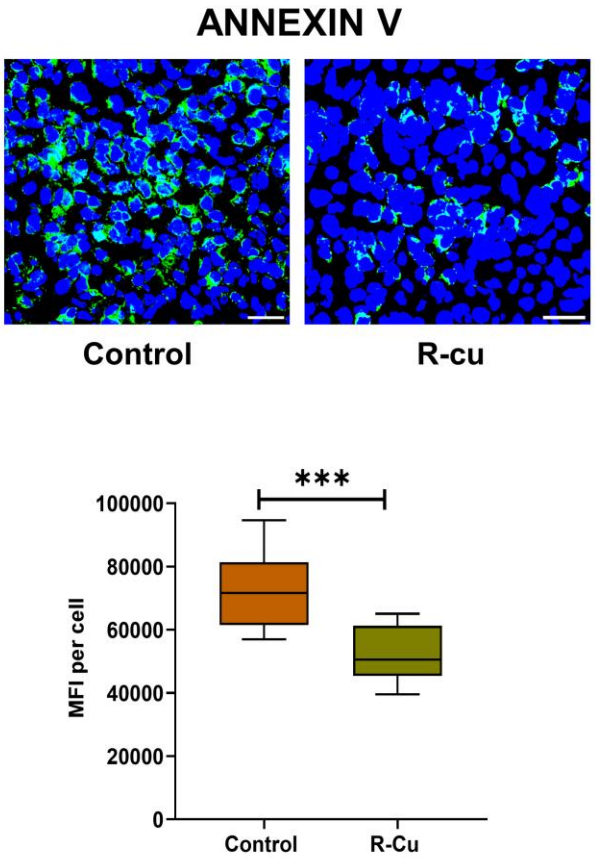

Figure S8: Representative IF images of Annexin V in control and R-Cu treated samples. Quantitative results are presented as boxplots. n = 10 each in control and R-Cu treated groups. *** = $p < 0.001$.

Table S1: Demographic information of control and Resveratrol and Copper (R-Cu) treated patients.

Table S2: List of biomarkers and antibodies used in this study.

Table S3 & S4: General information on RNA-seq data and a detailed list of differentially expressed genes